

Chemical and dynamical speciation of mobile ions in the glassy fast ionic conductor $\text{Ag}_2\text{S}+\text{B}_2\text{S}_3+\text{SiS}_2$: A ^{109}Ag nuclear magnetic resonance study

T. Akai* and S. W. Martin†

Department of Materials Science and Engineering, Iowa State University of Science and Technology, Ames, Iowa 50011-3114

F. Borsa

Department of Physics and Astronomy and Ames Laboratory, Iowa State University of Science and Technology, Ames, Iowa 50011-3160

(Received 19 January 1999; revised manuscript received 1 June 2000; published 18 December 2000)

^{109}Ag NMR in the highly conductive glass $0.525\text{Ag}_2\text{S}+0.475(0.5\text{B}_2\text{S}_3+0.5\text{SiS}_2)$ was investigated from 230 to 433 K. The ^{109}Ag NMR spectra reveal for the first time three well resolved lines corresponding to three kinds of chemically speciated Ag ions in sites with different chemical shifts in a macroscopically homogeneous glass. This chemical speciation of Ag ions is discussed in relation to the microstructure of the glass. As the temperature is increased, the three lines that originate from three different species of ions are narrowed, but these lines exist independently up to 433 K, the highest temperature measured. Nuclear spin-lattice relaxation rates (NSLR's), $1/T_1$, were also measured. Two relaxation processes were found; one is associated with two of the chemically speciated Ag ions and the other is associated with the other Ag ions. The two different NSLR's gradually approach a common value as the temperature is increased, and finally exhibit a common relaxation rate at and above 373 K. From the results of the NMR spectra and of the NSLR's, which observe the ion dynamics on different time scales, it is concluded that the silver ions move fast within separate clusters of similar chemical environments ($\gg\text{kHz}$), but exchange among the three different clusters at relatively slow rates ($\leq 100\text{ Hz}$) above 373 K. From the time the ions reside at any one site, the mean free path of the ions is estimated.

DOI: 10.1103/PhysRevB.63.024303

PACS number(s): 66.30.Hs, 76.60.-k

INTRODUCTION

Glassy ionic conductors have attracted much interest recently because of the tremendous decoupling of the dynamical timescale for ion motion, typically on the order of nanoseconds, from the timescale for structural relaxation (change) of the host network forming glass, typically on the order of geological time. Such decoupling enables ionic diffusion that rivals, and in some cases exceeds, that of ionic liquids.^{1,2} These high ionic conductivity values have prompted the consideration of their application in electrochemical devices such as ion-selective electrodes, solid-state batteries, and fuel cells. The advantages of glassy electrolytes over other electrolytes such as polymers are their higher single ion conductivity, typically cationic, and their electrochemical stability.

In the last two decades, much work has been done in the pursuit of even higher ionic conductivities. For example, it has been found that the ionic conductivity is progressively increased by using highly polarizable Ag ions,³ doping of the glass with alkali or silver halides,⁴ mixing of the glass formers,⁵ and the use of sulfide-based glasses.⁶ Unfortunately, it is found that selenide-based glasses, while being a logical extension of this chemical modification of glass, do not provide the increase in the ionic conductivity as might be expected.⁷ By a combination of these compositional optimization effects, the conductivity in glass can be increased from that of essentially nonconducting values of $\sim 10^{-10}(\Omega\text{ cm})^{-1}$ for simple alkali silicate glasses⁸ up to $\sim 10^{-2}(\Omega\text{ cm})^{-1}$ at room temperature for AgI-doped silver borate, silver phosphate, or silver germanate glasses, for example.⁹⁻¹¹ At this point, it appears that our recent work on the compositionally optimized AgI-doped $\text{Ag}_2\text{S}+\text{B}_2\text{S}_3+\text{SiS}_2$ glasses are among the most optimized of all glasses.^{12,13}

Although simple calculations¹⁴ predict that the highest conductivity would be in the range of $\sim 10^2(\Omega\text{ cm})^{-1}$, it appears that the ionic conductivity never reaches values above $\sim 10^{-2}(\Omega\text{ cm})^{-1}$ even in highly compositionally optimized glasses. The question naturally arises then is whether this value is the highest conductivity that can be achieved in glassy ionic conductors? If the glass composition has been optimized as far as is possible, what new underlying physics and materials chemistry lie at root of the cause of the limiting value of the conductivity? To begin to answer these questions, we return to some of the theories describing ion-transport mechanisms in glassy ionic conductors.

Many theories have been proposed to interpret the compositional dependence of the ionic conductivity in glass.¹⁵⁻¹⁷ In most models, the conductivity activation energy is divided into two terms, an electrostatic energy and a strain energy. These models have been successful in explaining the gross features of the relationships between the ionic conductivity and glass composition and in predicting new glass compositions with even higher conductivities, as already mentioned.^{4,6} While these particular models have been successful, they nonetheless deal with compositional and structural features that lie at the simplest short-range order level of glass.

Many researchers stress that the models of the conductivity should describe larger segments of the glass structure, out to at least the intermediate range, because ionic conduction involves the long range hopping of ions over multiple sites in the glass structure. One particular set of intermediate range order models are those based on the percolation of cation sites to form preferred, and hence lower energy, conduction pathways¹⁸⁻²¹ in the glass. This model suggests that doping of the glass either by a glass structure modifying oxide such

as an alkali oxide (M_2O), or by a structurally neutral dopant salt, such as AgI , creates preferred conduction pathways between *clusters* in the glass. This concept seems to be a natural one considering the tendency for many glass-forming liquids to heterogeneously phase separate on both microscopic and macroscopic levels. However descriptive these models are, they are nonetheless not easily proven. Even if the models were correct, fundamental questions about them and their veracity remain unanswered. For example, what are the microstructures like in these glasses? How fast do ions move in, between, and among these microdomains and how do these motions affect the macroscopically measured ionic conductivity?

In this paper, we report the first ^{109}Ag NMR results for a family of compositionally optimized silver sulfide thioborosilicate glasses previously investigated^{12,13} by ionic conductivity. In principle, ^{109}Ag NMR is informative in elucidating the complex chemical environment in glasses because it exhibits a large chemical shift that can be used to discriminate between different chemical environments. However, because of the poor signal-to-noise ratio, ^{109}Ag NMR in superionic glasses and crystals are relatively rare.^{22–28} In this first NMR study of these glasses, we report ^{109}Ag NMR measurements on ternary $Ag_2S+B_2S_3+SiS_2$ glasses that can distinguish different silver ions speciated not only by their unique chemical environment, but also by their different ionic mobilities, yielding new information about the formation of microstructures in these glasses.

EXPERIMENT

$Ag_2S+B_2S_3+SiS_2$ glasses were prepared from reagent grade Ag_2S and SiS_2 (99.9%, metals basis, Cerac, Inc.) and vitreous $B_2S_3(v-B_2S_3)$ prepared in our laboratory. The preparation procedure of $v-B_2S_3$ has been described elsewhere.²⁹ The glass batches of appropriate amounts of the starting materials were melted in a vitreous carbon crucible at $\sim 850^\circ C$ for ~ 15 minutes in an O_2 - and H_2O - free glove box and quenched by pressing the melt between brass plates. The samples were ground to a fine powder using an agate mortar and pestle and sealed under vacuum in a silica tube (7 mm OD). Powder x-ray diffraction was used to verify the amorphous nature of the glasses. Liquid-liquid phase separation has been observed for compositions lower in Ag_2S than the target composition and crystallization observed for compositions higher in Ag_2S than the target composition.¹³ Neither process was observed for the target composition used in this study.

The ^{109}Ag NMR experiments were performed using a phase coherent pulse Fourier transform (FT) home-built NMR spectrometer in connection with an 8.2T superconducting magnet. The resonance frequency was 16.259 MHz. In order to maximize the signal-to-noise ratio of the ^{109}Ag signal, a coil was designed to give high Q values of ~ 100 . This large Q value coil, however, caused long dead times due to ringing ($\sim 100 \mu s$), and for this reason the spectra were created by Fourier transforming the latter half of the echo signal obtained by a $(\pi/2)_x-t_1-(\pi/2)_y-t_1$ pulse sequence with $t_1=100 \mu s$. This sequence is usually used to

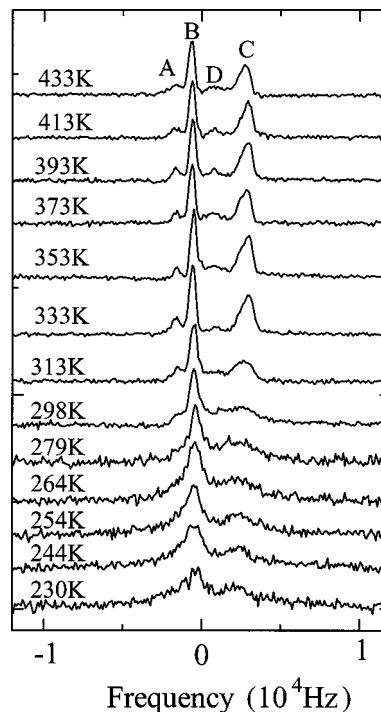


FIG. 1. ^{109}Ag NMR spectra for $0.525Ag_2S+0.475(0.5B_2S_3+0.5SiS_2)$ glass at different temperatures from 230 to 433 K. The spectra were obtained by $(\pi/2)_x-t_1-(\pi/2)_y-t_1$ methods.

observe solid echoes in solids where the free precession (fp) decay is dominated by short spin-spin relaxation times, T_2 , and the echo is observable only when the second pulse is given inside the fp decay. In the present case, the fp decay has a non-negligible contribution arising from the inhomogeneous broadening of the line (T_2^*) so that the echo can also be observed outside the fp decay (Hahn echo). With a $(\pi/2)_x-t_1-(\pi/2)_y-t_1$ sequence, the solid echo gives the same intensity as the free induction decay in the rigid case, while the Hahn echo gives half of it. What is observed here then is a mixture of the two kinds of echoes. In this case, therefore, the intensity of the spectra is not simply proportional to the number of resonating nuclei.

Because of the relatively long T_1 values and low signal-to-noise ratio for ^{109}Ag , the saturation-recovery method was used for the NSLR measurement to minimize the experimental time. After saturation by a long sequence of radio frequency (rf) pulses, the magnetization was measured as a function of recovery time. The measurement of M_z was obtained from the FT spectrum. The typical $\pi/2$ pulse was $\sim 20 \mu s$ long. Approximately 1600 FID's were accumulated. No thermal hysteresis was found in NMR data throughout these experiments.

RESULTS

Absorption spectra

Figure 1 shows the temperature dependence of the ^{109}Ag NMR spectra for the glass $0.525Ag_2S+0.475(0.5B_2S_3+0.5SiS_2)$. As can be seen in the spectra, the widths of the three NMR lines are motionally narrowed as the temperature

is increased. Among these three peaks, peak (C) undergoes narrowing at higher temperatures (~ 330 K), while peaks (A) and (B) are narrowed in the same lower temperature range (~ 260 K). A very weak line (D) is also discernible in the spectra and lies between lines (B) and (C). Above 333 K, the lines seem to have reached the limiting of narrowing and the spectra do not show any significant change with further increase in temperature. One interesting feature in this temperature range is that the narrowed three peaks are well resolved. This means that the motion of the silver ions is very rapid within each site (sufficiently fast to narrow the line), but there is no fast chemical exchange between the three different sites (sufficiently slow to inhibit chemical exchange and hence the averaging of the sites).

To chemically assign these three sites, samples were prepared with different thermal histories and chemical composition, and examined using ^{109}Ag NMR. In Fig. 2, the spectra are for $0.525\text{Ag}_2\text{S}+0.475(0.5\text{B}_2\text{S}_3+0.5\text{SiS}_2)$ at 298 K in a rapidly quenched (homogeneous) 2(a) and a slowly quenched (partially crystallized) 2(b) sample, respectively. Peaks (A) and (B) appear to shift downfield, whereas peak (C) appears to be little changed in peak position. We also measured the ^{109}Ag NMR spectra in samples with different composition. Ideally, one would want to measure the spectra of both $v-0.5\text{Ag}_2\text{S}+0.5\text{SiS}_2$ and $v-0.5\text{Ag}_2\text{S}+0.5\text{B}_2\text{S}_3$ to obtain good chemical shift references for silver ions in thiosilicate and thioborate environments, respectively. Unfortunately, the $\text{Ag}_2\text{S}+\text{SiS}_2$ system does not form glasses under normal rapid quenching conditions, so we were able to only prepare $v-0.5\text{Ag}_2\text{S}+0.5\text{B}_2\text{S}_3$. The ^{109}Ag NMR resonance in this glass gives a single peak at around the frequency of peak (B), Fig. 2(c). These results will be further discussed below to develop a structural model for these glasses.

NSLR measurements

Figure 3 displays the recovery of ^{109}Ag nuclear magnetization in the $0.525\text{Ag}_2\text{S}+0.475(0.5\text{B}_2\text{S}_3+0.5\text{SiS}_2)$ glass at 230, 244, 279, and 298 K. The recovery of $M_z(t)$ after satu-

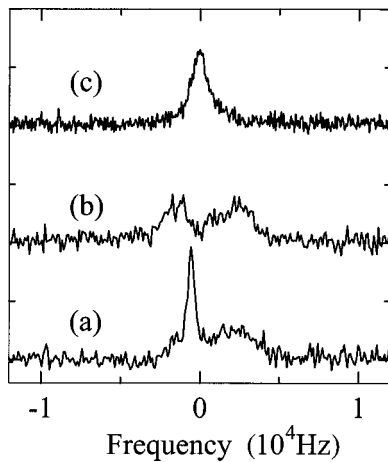


FIG. 2. ^{109}Ag NMR spectrum in (a) rapidly quenched $0.525\text{Ag}_2\text{S}+0.475(0.5\text{B}_2\text{S}_3+0.5\text{SiS}_2)$, (b) slowly quenched $0.525\text{Ag}_2\text{S}+0.475(0.5\text{B}_2\text{S}_3+0.5\text{SiS}_2)$, and (c) slowly quenched $0.5\text{Ag}_2\text{S}+0.5\text{B}_2\text{S}_3$.

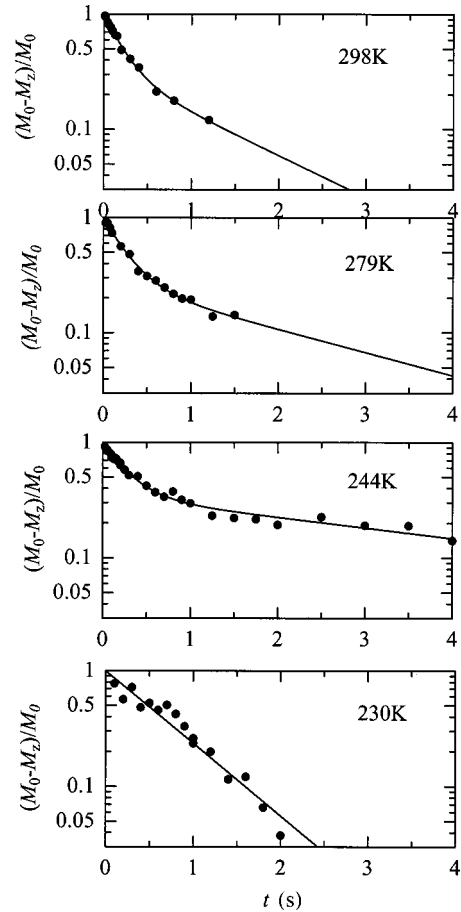


FIG. 3. Semi-log plot of the recovery of the ^{109}Ag nuclear magnetization M_z for $0.525\text{Ag}_2\text{S}+0.475(0.5\text{B}_2\text{S}_3+0.5\text{SiS}_2)$ glass at 230, 244, 279, and 298 K. At 230 K, it was impossible to measure the longer relaxation time, so that only the shorter relaxation time was measured.

ration for nuclear spin $I = \frac{1}{2}$ should be expressed as a single exponential if all nuclei have a common spin temperature

$$\frac{M_z(\infty) - M_z(t)}{M_z(\infty)} = \exp(-t/T_1). \quad (1)$$

As Fig. 3 shows, below ~ 298 K, deviation from single-exponential recovery was found. Such a nonexponential recovery has also been found in $0.7\text{Li}_2\text{S}+0.3\text{B}_2\text{S}_3$ glasses.³⁰ Observing the time evolution of the recovery of the spectra after the saturation of rf pulses at 298 K, we found that lines for the (A)+(B) sites show similar recovery, while line (C) relaxes at a much slower rate as shown in Fig. 4(a). Hence, we attribute the nonexponential recovery to the different NSLR's from the different chemical environments for the silver ions. Since the separate measurements of $1/T_1$ for the different sites by evaluating the areas under the different peaks is uncertain at low temperatures, we decided to separate the relaxation rates of the different sites by fitting the recovery of the area of the whole spectrum using the expres-

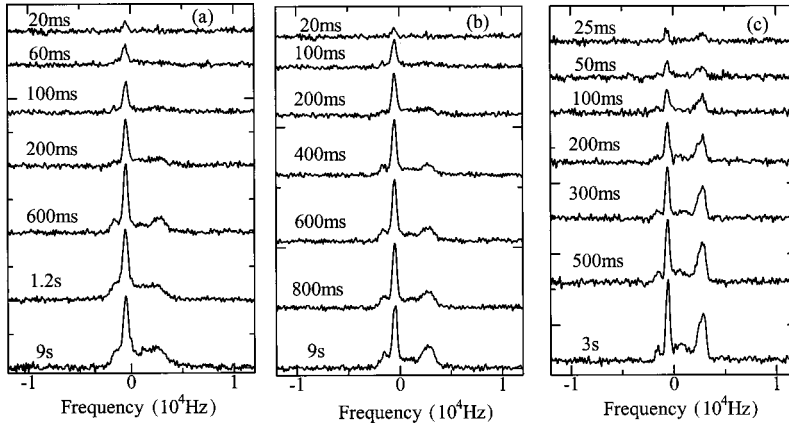


FIG. 4. ^{109}Ag magnetization recovery after the saturation by rf pulse in $0.525\text{Ag}_2\text{S} + 0.475(0.5\text{B}_2\text{S}_3 + 0.5\text{SiS}_2)$ at (a) 298 K and (b) 313 K, and (c) 373 K. The recovery times are shown in the figures.

$$\frac{M_z(\infty) - M_z(t)}{M_z(\infty)} = f' \exp(-t/T_1') + (1 - f') \exp(-t/T_1''), \quad (2)$$

where $1/T_1'$ and $1/T_1''$ are the NSLR's of sites (A)+(B) and site (C), respectively, and f' and $f'' = (1 - f')$ are the fractions of the contribution of each of these to the magnetization recovery. f' , $1/T_1'$, and $1/T_1''$ were obtained by fitting the recovery curve by the least-squares method. To examine whether two T_1 's (T_1' and T_1'') thus obtained measure the different relaxation rates in the (A)+(B) and (C) sites, respectively, we compared them with the $1/T_1$ obtained from the recovery of the intensities of peaks (B) and (C) separately at 298 K. It was found that these two $1/T_1$ values so obtained are approximately similar, which justifies the procedure used.

At 313 K, these two sites still give a different relaxation behavior as shown in Fig. 4(b). Since the lines are narrowed, it was possible to integrate the spectra of the (A)+(B) and (C) sites separately to obtain each area. In Fig. 5, the recovery of the area of sites (A)+(B) (closed circles) and of site (C) (open circles) are plotted along with that of the total area (crosses). The normalized magnetization from the total spectrum (crosses) approaches a single exponential decay. This behavior is probably due to the fact that the T_1 values become closer in magnitude. It is seen that the recovery rates for the (A)+(B) and (C) sites become similar with the increase in temperature and eventually coincide at 373 K to give a common $1/T_1$ value above this temperature. Above 373 K (up to 433 K), all of the magnetization relaxes with the same relaxation rate as illustrated in the recovery spectrum shown in Fig. 4(c). This common T_1 shows a slight tendency to increase as the temperature is increased as can be noted at the bottom of Fig. 5.

The temperature dependence of the ^{109}Ag $1/T_1$ for the two sites is shown in Fig. 6. The faster $1/T_1$ [closed circles, sites (A)+(B)] exhibits a very weak temperature dependence. This behavior has been found in other silver conducting glasses.^{24,25,28} A most interesting feature in this figure is that two different $1/T_1$'s at low temperature gradually approach a common value as temperature is increased and a common $1/T_1$ is observed above 373 K.

In summary, two relaxation processes were found in the ^{109}Ag NMR NSLR's. These two sites have different $1/T_1$

values below 298 K. These two different $1/T_1$ values approach a common value as the temperature is increased, and finally a single relaxation rate $1/T_1$ is measured above 373 K.

DISCUSSION

Chemical speciation in fast ion conducting glasses

We begin by discussing the origin of the three peaks observed in the ^{109}Ag NMR spectra. As mentioned above, the motion of the Ag ions is fast enough to average out magnetic

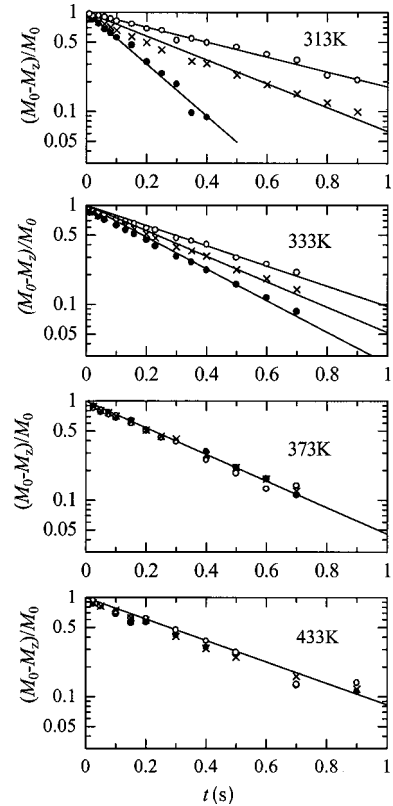


FIG. 5. Semi-log plot of the recovery of the ^{109}Ag nuclear magnetization for $0.525\text{Ag}_2\text{S} + 0.475(0.5\text{B}_2\text{S}_3 + 0.5\text{SiS}_2)$ glass at 313, 333, 373, and 433 K. Open circles show those from the area of the peak in the right-hand side (C). Closed circles show those from the area of the peaks from the left-hand side [(A)+(B)]. Crosses show those from the total area of the spectrum.

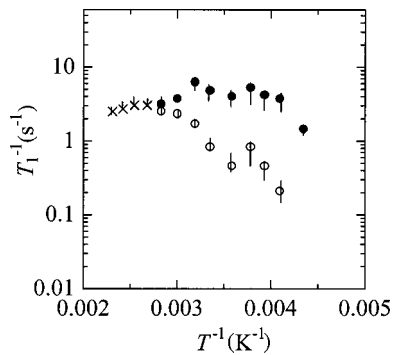


FIG. 6. Temperature dependence of $^{109}\text{Ag } T_1$ for $0.525\text{Ag}_2\text{S} + 0.475(0.5\text{B}_2\text{S}_3 + 0.5\text{SiS}_2)$ glass. Open circles are obtained from peak (C). Closed circles are obtained from (A) and (B). These two different $1/T_1$'s merge into a common value above 373 K as shown as crosses.

inequivalency or anisotropy in each site. Since a local vibrational mode would not be able to average out the site anisotropy, the fast motion of the ions must extend out in distance, at least more than a single chemical bond, for example. On the other hand, the motion must be restricted in distance since three separate resonance lines are observed. Therefore, the ions must be moving fast within domains of different chemical environments in the glass. There have been previous examples of this behavior, such as that in the work by Villa *et al.*²⁶ They observed multiple resonance peaks in a Ag-I doped $\text{Ag}_2\text{O}-\text{B}_2\text{O}_3$ glass from what they hypothesized as different domains in glass. As shown in Fig. 2(b), the Ag absorption peaks in our glasses also become more differentiated with heat treatment, which strongly support the view that the different sites observed in Fig. 2 arise from domains with different chemical environments in the glass.

The question becomes then, what is the origin of the difference in the averaged chemical environment that gives rise to three separate resonance peaks? Since the chemical shift of Ag is known to be very large (1000 ppm, ≈ 16 kHz),³¹ the differences in the resonance frequencies must be associated with the averaged chemical shift differences of the three various sites. The best way to identify these peaks would be to compare the chemical shifts observed with those of the corresponding crystals whose short-range structures are known and well defined. Unfortunately, due to the uniqueness of the phases being studied here, neither the chemical shifts nor the corresponding phases are known at present and as such we cannot completely assign these peaks. However, we can suggest on the origin of the chemical shift differences by considering the possible short-range structures of Ag ions based on the results as shown in Fig. 2 and previous studies.

Our work on the structure of alkali thio borate glasses has shown that in similarity to the oxide borate glasses, these glasses exhibit the formation of tetrahedral borons and trigonal borons with varying numbers of nonbridging sulfurs bonded to them.³² Our preliminary ^{11}B NMR (Ref. 33) and Fourier transform infrared (FTIR) studies³⁴ of $v-0.5\text{Ag}_2\text{S}+0.5\text{B}_2\text{S}_3$ shows that a large fraction the borons in the glass are four coordinated. Further, we³⁵ and Eckert *et al.*³⁶ have shown that in alkali thiosilicate glasses, the silicon is tetrahedrally coordinated by sulfurs and that the frac-

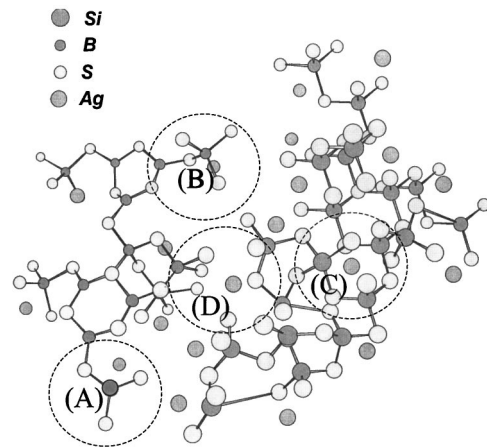


FIG. 7. Proposed model for the structure of the three domains, (A), (B), (C), and (D), observed in ^{109}Ag NMR spectrum. Sites (A) are silver ions bonded to nonbridging sulfur anions connected to trigonal borons. Sites (B) are silver ions bonded to bridging sulfurs connected to tetrahedral borons. Sites (C) are silver ions bonded to nonbridging sulfur anions connected to tetrahedral silicons. Possible sites (D) would be silver ions located interstitially between these domains. Note that circle describes only chemical association, not the size of the domain.

tion of nonbridging sulfurs increases with modifying alkali sulfide content. The thiosilicate tetrahedral units have a strong propensity for sharing edges rather than corners.³⁶ Ag^+ ions bonded to the thiosilicate part of the glass structure will therefore be bonded to nonbridging sulfurs, in turn, bonded to silicon atoms at the center of edge sharing tetrahedra. These studies show, therefore, that there are two possible units for the coordination of Ag: Ag bonded to thio borate units and Ag bonded to thiosilicate unit. In addition to this, we suggest the possibility that the Ag ions are equally shared between these two structural subsets based upon our recent studies of alkali borosilicate glasses.³⁷

Returning to the fact that we see a single absorption peak in the $0.5\text{Ag}_2\text{S}+0.5\text{B}_2\text{S}_3$ glass close to the position of (A)+(B) peaks in the ternary glasses, it is very likely that these two peaks are from Ag^+ associated with thio borate units and peak (C) is from Ag^+ associated with thiosilicate units. The origin of the difference in (A) and (B) is not clear at present. However, from the above arguments, it may be appropriate to associate the origin of minor difference of (A) and (B) to minor differences of chemical bonding of Ag bonded to thio borate units, i.e., four coordinated (B) or three coordinated borons (A). Site (D), lying between (A)+(B) and (C), may be associated with Ag^+ ions residing in an “interface” region between (A)+(B) and (C) microstructures. Hence, we propose a model as depicted in Fig. 7. It should be noted that the figure shows only chemical association of each site and it does not show any information on the size or the shape of each domain.

Dynamical speciation in fast ion conducting glasses

The lines (A)+(B) are motionally narrowed at a lower temperature compared to that of line (C). It is also found that the silver ions residing, on average, in site (A)+(B) yield a

broad $1/T_1$ maximum at a lower temperature than the $1/T_1$ maximum of the ions in site (C) (see Fig. 6). These facts indicate that the Ag^+ in (A)+(B) and (C) which are distinctly chemically speciated, as discussed above, have dynamical speciation as well. The $1/T_1$ measurements further indicate that the ions in (A)+(B) sites exhibit faster ion dynamics than those in the (C) sites.

The question naturally arises as to whether the faster motion of ions residing in the (A)+(B) sites is associated with ionic conduction. To examine whether they are related, we compare the diffusion constants calculated from the ionic conductivity (D_σ) and that calculated from the NMR $1/T_1$ measurements (D_{NMR}). From the Nernst–Einstein equation,

$$D_\sigma = \frac{\sigma kT}{N_i e^2}, \quad (3)$$

where k is the Boltzmann factor, T is temperature, N_i is number density of mobile ions, and e is the charge of electron. Substituting $N_i = 1.7 \times 10^{28} \text{ m}^{-3}$, $\sigma = 5.0 \times 10^{-3} (\Omega \text{ cm})^{-1}$, Ref. 12, we get $D_\sigma = 4.7 \times 10^{-12} \text{ m}^2/\text{s}$ at 298 K. From the Einstein equation, D_{NMR} can be expressed as,

$$D_{\text{NMR}} = \frac{r^2}{6\tau_c}. \quad (4)$$

The mean jump distance, r , is found to be ~ 0.4 nm from the density, assuming a homogeneous distributions of ions. The chemical inhomogeneity described above refers to the anion structure, not the mobile cations. The $1/T_1$ data shown on Fig. 6 exhibits a broad maximum that is centered in the vicinity of room temperature. In this case, we can directly use the relation $\omega_0 \tau_c = 0.64$, when $1/T_1$ is at its maximum. As such, τ_c becomes $\sim 6.3 \times 10^{-9}$ s and using Eq. (4) D_{NMR} is calculated to be $4.2 \times 10^{-12} \text{ m}^2/\text{s}$. Since these two diffusion coefficients are similar, this suggests that the motions of ions in this domain may be associated with ionic conductivity.

So far, we have discussed the dynamic speciation of chemically speciated ions, but on the other hand, it is very likely that these ions moving fast within a domain are perfectly isolated and do not exchange at all. In the following, we discuss whether there exists interdomain exchange between these silver ions based on the $1/T_1$ results described earlier.

At low temperature (below 298 K), spins in the (A)+(B) sites have different spin-temperatures after the saturation by the irradiation of the pulse from that of the spins in the (C) sites. This means that the two spin subensembles [(A)+(B) and (C)] are energetically isolated, i.e., the cross relaxation (CR) time τ_{CR} between these two sites fulfills the condition $1/\delta\omega \approx 5 \times 10^{-5} \text{ s} \ll T_1 \approx 1 \text{ s} \ll \tau_{\text{CR}}$. As already described, the two T_1 's of these sites merge gradually above room temperature and finally a common T_1 is observed at 373 K. From 373 to 433 K, only a single T_1 is observed. One possibility of this behavior is simply that the two sites happen to have the same relaxation time T_1 above 373 K. This coincidence is unlikely since T_1 remains unique over a wide temperature range (see Fig. 6). The second possibility, which we will

assume here, is that the two sites acquire a common T_1 because the condition $1/\delta\omega \approx 5 \times 10^{-5} \text{ s} \ll \tau_{\text{CR}} \ll T_1 \approx 1 \text{ s}$ is fulfilled.

There are two possible mechanisms for the cross-relaxation between these sites. The first is the chemical exchange of ions between the (A)+(B) and (C) sites and the second is spin diffusion between the sites. We favor the chemical exchange mechanism between the two sites because spin diffusion is not enhanced as the temperature is increased, while chemical exchange, viz., ion diffusion among the sites, is promoted at higher temperature. From the T_1 behavior, then, we suggest that *interdomain* diffusion does exist although it is slow; and occurs on a time scale of T_1 (\sim Hz), but also that it is much slower than chemical shift difference (\sim kHz).

Given the fact that the mobile silver ions have fast *intra-domain* motion and a relatively slow *interdomain* motion, we now use NMR measurements to estimate both the resident time the ions spend, on average, in each domain, as well as the mean free-path (a measure of the distance the ion travels in a random walk during the residence time) for intradomain motion.

At the upper temperature range of our measurements, >373 K, where the silver ions have a common T_1 , the time spent by any one Ag^+ ion in a given cluster or domain, lies between T_1 , ~ 0.3 s and the inverse of the chemical shift difference between the two sites, $1/(2\pi\delta f)s \approx 0.00005$ s. Hence, $t \sim 0.001$ s is a plausible estimate for the resident time of any one silver cation in a given domain or cluster. Assuming a three-dimensional diffusion model,³⁸ the mean displacement distance l is expressed as,

$$l = \sqrt{6Dt}, \quad \text{where } D = \frac{r^2}{6\tau_c}f, \quad (5)$$

and r is the jump distance and f is the correlation factor. As above, the jump distance (~ 0.4 nm) was calculated from the density assuming the Ag ions are homogeneously distributed in the glass. f is taken as 0.3 which is often found in glasses with high ionic concentration.³⁹ As seen in Fig. 6, at higher temperatures, the NSLR is not strongly temperature dependent and suggests a similar weak temperature dependence to τ_c . Hence, τ_c is assumed to be the same as that at 298 K calculated before to be 6.3×10^{-9} s. Substituting these values into Eq. (7), l is calculated to be 87 nm ($10 < l < 200$ nm). This distance calculated here is in general agreement with the length scales for diffusional domains as determined by neutron scattering among other techniques.⁴⁰

At present, it is not clear how the mean free path thus obtained corresponds to the domain size of the thioborate glass structure in which the (A)+(B) sites reside. All that can be concluded from the present measurements is that the Ag ions residing in these sites diffuse on average 87 nm before their spin energy is relaxed. We are currently using neutron scattering and other techniques more sensitive to long-range structure in glass to examine the actual sizes of these regions. In particular, we are carefully examining the possibility that these glasses are phase separated on a very small length scale and as such may be at the root of the cause for both chemical

and dynamical speciation of the mobile Ag cations. Our preliminary work, however, does not support these glasses as being phase separated.⁴¹

CONCLUSION

¹⁰⁹Ag NMR was investigated in the superionic glass, 0.525Ag₂S+0.475(0.5B₂S₃+0.5SiS₂). The temperature dependence of the spectra revealed for the first time that there exist at least three silver cation environments in these glasses which are speciated both by their different chemical environments as well as by their different ion dynamics. It is found that the ion diffusion within each domain is rapid compared to the exchange rate of silver cations between the different domains. By comparing the diffusion coefficients calculated from both the ionic conductivity and the NMR data, the ionic conduction is associated with the fast *intradomain* diffusion where ionic motions are more rapid. From the combination

of the NMR line shape analysis and the relaxation rate data, it is estimated that the mean residence time in each domain is on the order of 10⁻³ s just above 373 K.

ACKNOWLEDGMENTS

T.A. thanks the Atomic Energy Bureau of Science and Technology Agency of Japan for supporting her visit at Iowa State University. Zehoon Jang and Eric Lee are especially thanked for their assistance with NMR measurements. Jeremy Schrooten and Mike Royle are thanked for their help in the preparation and characterization of the glasses. This research was supported in part by a grant from the National Science Foundation, NSF-DMR 94-20561 (S.W.M.). Ames Laboratory is operated for the U.S. Department of Energy by Iowa State University under Contract No. W-7405-Eng82. This work was partially supported by the Director for Energy Research, Office of Basic Energy Sciences (F.B.).

*On leave from Osaka National Research Institute, AIST, Ikeda, Osaka, Japan.

†Author to whom correspondence should be addressed.

¹C. A. Angell, *Solid State Ionics* **18/19**, 72 (1986).

²C. A. Angell, *Annu. Rev. Phys. Chem.* **172**, 1 (1992).

³G. Robert, J. P. Malugani, and A. Saida, *Solid State Ionics* **3/4**, 311 (1981).

⁴A. Levasseur, J. C. Brethous, J. M. Reau, and P. Hagenmuller, *Mater. Res. Bull.* **14**, 921 (1979).

⁵A. Magistris, G. Chiodelli, and M. Villa, *J. Power Sources* **14**, 87 (1985).

⁶A. Levasseur, R. Olazcuaga, M. Kbala, M. Zahir, and P. Hagenmuller, *C. R. Seances Acad. Sci., Ser. 2* **293**, 563 (1981).

⁷V. Michel-Lledos, A. Pradel, and M. Ribes, *Eur. J. Solid State Inorg. Chem.* **29**, 301 (1992).

⁸H. L. Tuller, D. P. Button, and D. R. Uhlmann, *J. Non-Cryst. Solids* **40**, 93 (1980).

⁹A. Pradel and M. Ribes, *Mater. Sci. Eng., B* **3**, 45 (1989).

¹⁰A. Pradel and M. Ribes, *Mater. Chem. Phys.* **23**, 121 (1989).

¹¹S. W. Martin, *J. Am. Ceram. Soc.* **74**, 1767 (1991).

¹²J. Kincs and S. W. Martin, *Phys. Rev. Lett.* **76**, 70 (1996).

¹³J. Kincs, M. S. thesis, Iowa State University, 1994.

¹⁴T. Minami, *J. Non-Cryst. Solids* **73**, 273 (1985).

¹⁵D. Ravain and J. L. Souquet, *Phys. Chem. Glasses* **18**, 27 (1977).

¹⁶O. L. Anderson and D. A. Stuart, *J. Am. Ceram. Soc.* **37**, 574 (1954).

¹⁷S. W. Martin, *J. Am. Ceram. Soc.* **71**, 438 (1988).

¹⁸S. W. Martin, *Solid State Ionics* **51**, 19 (1992).

¹⁹(a) A. Bunde, P. Maass, and M. D. Ingram, *Ber. Bunsenges. Phys. Chem.* **95**, 977 (1991); (b) K. Funke, B. Roling, and M. Lange, *Solid State Ionics* **105**, 195 (1998).

²⁰M. Mangion and G. P. Johari, *Phys. Rev. B* **36**, 8845 (1987).

²¹M. D. Ingram, M. A. MacKenzie, W. Muller, and M. Torge, *Solid State Ionics* **40/41**, 671 (1990).

²²P. Sanz, R. Herrero, S. Rojas, S. Rojo, J. M. Rossignol, J. M. Reau, and B. Tanguy, *Solid State Ionics* **82**, 129 (1995).

²³K. Olsen and J. W. Zwanziger, *Solid State Nucl. Magn. Reson.* **5**, 123 (1995).

²⁴S. W. Martin, H. J. Bischof, M. Mali, J. Roos, and D. Brinkmann, *Solid State Ionics* **18/19**, 5 (1986).

²⁵J. Roos, D. Brinkmann, M. Mali, A. Pradel, and M. Ribes, *Solid State Ionics* **28/30**, 12 (1988).

²⁶M. Villa, G. Chiodelli, A. Magistris, and G. Licheri, *J. Chem. Phys.* **85**, 2392 (1986).

²⁷K. Olsen, J. Zwanziger, P. Hartmann, and C. Jager, *J. Non-Cryst. Solids* **222**, 199 (1997).

²⁸S. H. Chung, K. R. Jeffrey, J. R. Stevens, and L. Borjesson, *Phys. Rev. B* **41**, 6154 (1990).

²⁹S. W. Martin and D. R. Bloyer, *J. Am. Ceram. Soc.* **73**, 3481 (1990).

³⁰H. Kim, D. R. Torgeson, F. Borsa, and S. W. Martin, *Solid State Ionics* **90**, 29 (1996).

³¹D. Brinkmann, *Prog. Nucl. Magn. Reson. Spectrosc.* **24**, 527 (1992).

³²See, for example, S. J. Hwang, C. Fernandez, J. P. Amoureux, J. W. Han, J. Cho, S. W. Martin, and M. Pruski, *J. Am. Chem. Soc.* **120**, 7337 (1998) and references therein.

³³J. A. Sills, J. Kincs, and S. W. Martin (unpublished).

³⁴A. Burns, and S. W. Martin, *J. Non-Cryst. Solids* (to be published).

³⁵S. W. Martin and J. A. Sills, *J. Non-Cryst. Solids* **135**, 171 (1991).

³⁶H. Eckert, J. H. Kennedy, A. Pradel, and M. Ribes, *J. Non-Cryst. Solids* **113**, 287 (1989).

³⁷S. W. Martin, J. MacKenzie, A. Bhatnagar, S. Bhowmik, and S. Feller, *Phys. Chem. Glasses* **36**, 82 (1995).

³⁸See, for example, F. Fusco and H. Tuller, in *Superionic Solids and Solid Electrolytes*, edited by A. Laskar and S. Chandra (Academic Press, Boston, 1989), p. 43.

³⁹S. Chandra, *Superionic Solids: Principles and Applications* (North-Holland, New York, 1981), pp. 232ff.

⁴⁰J. Swenson, L. Borjesson, and W. S. Howells, *Phys. Scr., T* **57**, 117 (1995).

⁴¹A. Matic, J. Swenson, L. Börjesson, S. Longeville, R. Lechner, W. S. Howells, T. Akai, and S. W. Martin, *Physica B* **226**, 69 (1999).